

# Simultaneous short and long range surveillance of drones and aircrafts with DVB-T based Passive Radar

Tatiana Martelli, Fabiola Colone  
DIET Dept. Sapienza, University of Rome  
Via Eudossiana 18, 00184 Rome, Italy  
{tatiana.martelli, fabiola.colone}@uniroma1.it

Roberta Cardinali  
Leonardo Company  
Via Tiburtina Km 12.400, 00131 Rome, Italy  
roberta.cardinali@leonardocompany.com

**Abstract** — In this paper, we consider the exploitation of a DVB-T based Passive Radar for simultaneous short and long range surveillance of drones and aircrafts, respectively. In detail, an airport terminal area surveillance application is considered and the effectiveness of the employed sensor is investigated with reference to the two search tasks to be accomplished simultaneously. For the purpose of our analysis, experimental data have been collected by means of the DVB-T based AULOS® passive sensor developed by Leonardo S.p.A against both a very small RCS drone and conventional air traffic. Then, an appropriate processing scheme is extensively applied against the collected datasets, based on the algorithmic solutions proposed by the research group at Sapienza University. The reported results preliminarily demonstrate the capability of a DVB-T based Passive Radar of simultaneously detecting and localizing drones flying around the airport area as well as the typical civil aircrafts at longer distances.

**Keywords**— *Passive Radar, DVB-T signals, drone detection, airport surveillance.*

## I. INTRODUCTION

In recent years, the research and development activities focused on Passive Radar (PR) have been astonishing in number, diversity, and worldwide distribution. One of the main drivers may have been the availability of affordable enabling technologies for both data capturing and processing, which allowed different stakeholders to engage in the emerging research. The reduced cost, the lack of additional electromagnetic pollution, and the inherently covert operation are some of the well-known advantages offered by PR, which make it an appealing solution for both civilian and military applications [1].

In this paper, we focus on a specific advantage provided by the PR operation that is the capability to provide simultaneous short and long range surveillance. Usually, such tasks are carried out by dedicated conventional radar systems, being the employed waveforms, the power budget, and the search strategies carefully tailored to the considered application.

Thanks to the intrinsic bistatic configuration and the parasitic exploitation of continuous wave (CW) transmitters, PR sensors do not suffer from blind ranges effect typical of active monostatic pulse radar. Moreover, the stationary nature and the isotropic characteristic of many of the employable illuminators of opportunity potentially allow us to exploit very long integration times on receive to compensate for the limited power

density provided by the emitter. This certainly applies to many ground-based transmitters for analog or digital radio/TV broadcasting. By continuously emitting their signals, these transmitters provide a persistent illumination of the targets of interest. Finally, based on the employed software-defined radio (SDR) receiver architecture, the signal processing is entirely digital and can be flexibly adapted to meet the requirements of different search tasks. These considerations suggest that PR could be a suitable sensor for the detection of small RCS targets at short ranges along with medium/big sized targets at farther distances. This could be an invaluable characteristic in several surveillance scenarios such as coastal areas and airport terminal/surface areas, where a variety of targets of interest are typically present at quite different ranges.

Among the considered waveforms of opportunity, digital broadcast transmitters, such as the DVB-T, are particularly attractive for applications requiring simultaneous short and long range surveillance. For instance, DVB-T based PR has been successfully employed for surveying the typical maritime traffic up to very long distances (even over the standard radar horizon) and, simultaneously, for monitoring small boats (namely, fishing vessels, rubber boats, etc.) in the proximity of the coast, [2]-[4].

The use of a DVB-T based PR could be a very effective solution also for airport terminal area surveillance. In such a scenario, in addition to the surveillance of the conventional air traffic, all the aircrafts and vehicles moving on the surface as well as possible threats in the proximity of the airport should be quickly detected. In particular, low flying objects such as Unmanned Air Vehicles (UAVs) and drones are becoming a serious threat for the aviation safety and the airport security. Recently, different collisions between aircrafts and drones have occurred and, more and more often, drones are sighted over the airport area causing the instant interruption of hundreds of scheduled flights and a huge inconvenience to the travellers [5]. Consequently, detection, tracking and classification of these particular objects have become key requirements for surveillance systems to protect airports and even critical national infrastructures from hostile incursions. A number of studies demonstrated the effectiveness of the DVB-T based PR technology for Air Traffic Control (ATC) applications [3],[6]-[7]. More recently, also the possibility of employing the considered sensor for detecting drones and small UAVs has been investigated in [8]-[10].

In this work, we explore the possibility to employ a single DVB-T based PR system in airport surveillance applications to

simultaneously detect and localize drones and aircrafts at short and long ranges, respectively. For the purpose of our analysis, dedicated acquisition campaigns have been performed in a military airport using the DVB-T based AULOS® passive sensor developed by Leonardo S.p.A. A very small cooperative drone was employed, flying in the surrounding area of the airport; in addition, aircrafts of civil air traffic have been considered as targets of opportunity at distances up to few hundreds of kilometers. An appropriate processing scheme, tailored for the twofold search task, has been implemented and extensively tested by the research group of Sapienza University. The results are reported both in terms of raw detection capability and after a localization/tracking stage.

The paper is organized as follows. In Section II, we present the scenario of interest. Section III describes the experimental test campaigns and the adopted processing scheme for target detection and localization whereas the obtained results are reported and illustrated in Section IV. Finally, Section V summarizes the main conclusions.

## II. AIRPORT TERMINAL AREA SCENARIO

Nowadays, due to the high-density traffic around the airport area, modern ATC and ground control systems are required to strengthen the airspace safety level and to enhance the security level in the proximity of an airport. It is necessary to accurately detect and track the conventional air traffic also during the landing and take-off phases. Moreover, a careful surveillance of the terminal area is required to prevent collisions and to avoid runway incursions from other aircrafts, vehicles or people. In addition, the recent increase of the number of UAVs and drones represents a further threat for airport security.

In the context outlined above, radar systems play an important role thanks to their long-range and all-weather, night and day monitoring capabilities. However, it is worth noticing that drone detection represents a challenging task for any radar system due to their complex motion, along with the small RCS and low velocity. Therefore, the surveillance level enabled by the conventional active radar systems could be augmented by the cost-effective and eco-friendly PR technology. In fact, in order to guarantee a complete and continuous coverage, PR can be effectively integrated within conventional active radars to extend the surveillance coverage, acting as “gap-filler”, but also to reduce the probability of out of service of the surveillance system. It is worth noticing that, aiming at the monitoring of airport terminal areas, where electromagnetic emissions are limited by regulations related to public safety and risk of interference with pre-existing systems, a network of passive sensors could be easily deployed to provide continuous and complete coverage.

Among the different waveforms of opportunity, the exploitation of the DVB-T transmitters represents one of the best choice for the considered application. In fact, the high radiated power of these transmitters and the excellent coverage make them suitable for the detection of small Radar Cross Section (RCS) and low-altitude targets as well as for

medium/long range air traffic surveillance applications. In addition, the continuous emissions and the good range resolution of about 40 m (thanks to the bandwidth of approximately 8 MHz) make the resulting PR potentially able to adapt the coherent integration time in order to continuously detect and discriminate multiple closely spaced targets. Eventually, by employing an OFDM modulation, the DVB-T signals are noise-like waveforms; thus, they provide ambiguity function with attractive properties that are nearly independent of the signal content and almost time-invariant [11].

In order to provide a preliminary evaluation of the expected coverage of such sensors against drones and aircrafts, a power budget analysis has been conducted. By resorting to the well-known bistatic radar equation [12], the signal-to-noise ratio (SNR) for a given target can be expressed as:

$$SNR = \frac{EIRP \cdot G_{RX} \cdot \lambda^2 \cdot \sigma}{(4\pi)^3 \cdot R_{TX}^2 \cdot R_{RX}^2 \cdot KT_0FB} G_{int} \quad (1)$$

Table 1 provides explicit definitions and values adopted for the parameters appearing in eq. (1). Notice that the numerical values as well as the bistatic radar geometry have been selected to be identical or close enough to those characterizing the experimental tests reported in Sections III and IV.

Fig. 1(a-b) show the expected SNR map across the surveyed area when a big sized target (RCS=100 m<sup>2</sup>) and a small RCS target (RCS=0.01 m<sup>2</sup>) are considered, respectively. In both case studies, we report the results over a square region of variable dimensions, where the position of the RX sets the axes origin and the TX lies at (X, Y) = (20.8, 11.3) km.

By observing Fig. 1(a) we notice that, in principle, aircrafts could be detected up to several tens of kilometers from the receiver with a high probability of detection for typical values of probability of false alarm ( $P_{fa}$ ). Simultaneously, based on the SNR values in Fig. 1 (b), small drones flying around the airport area could be detected with good probability up to 4-5 kilometers from the PR sensor.

Table 1 - Values used in the SNR simulation.

Parameters	Values
Equivalent Isotropic Radiated Power (EIRP)	50 kW
Receiver antenna gain ( $G_{RX}$ )	15 dB
Wavelength ( $\lambda$ )	0.525 m
Aircraft target RCS ( $\sigma$ )	100 m <sup>2</sup>
Drone target RCS ( $\sigma$ )	0.01 m <sup>2</sup>
Coherent processing gain ( $G_{int}@T_{int} = 1.2 s$ ) - aerial case	70.4 dB
Coherent processing gain ( $G_{int}@T_{int} = 0.5 s$ ) - drone case	66.6 dB
Noise figure, including system loss ( $F$ )	25 dB
Receiver bandwidth (B)	7.61 MHz
System temperature ( $T_0$ )	290 K

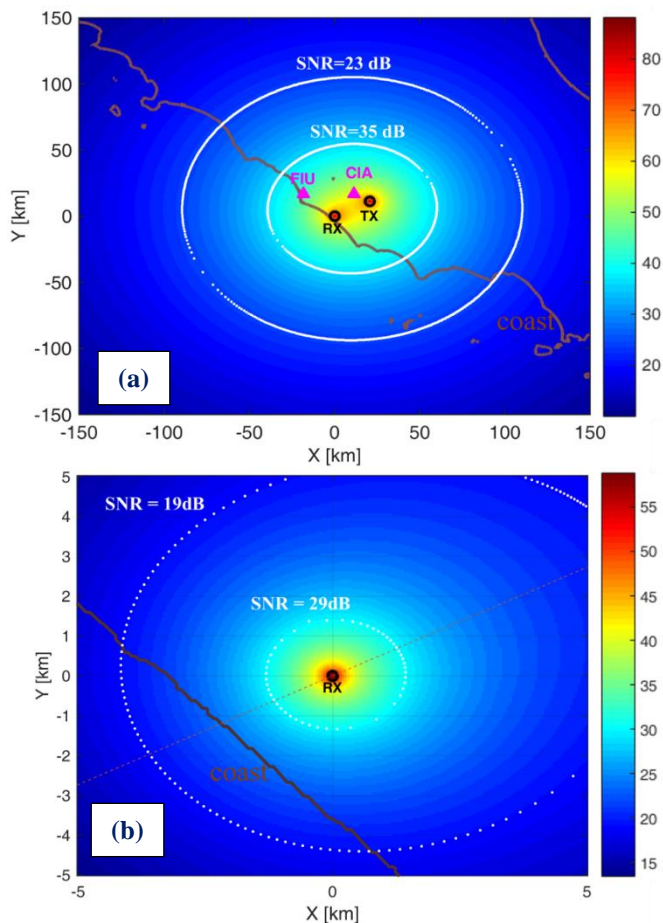


Fig. 1. Theoretical SNR at different distances from the DVB-T based PR against: (a) big sized aircrafts; (b) small drones.

It is worth mentioning that this analysis does not take into account the direct signal from the TX and the returns from the stationary scene, assuming ideally that these contributions have been perfectly removed by dedicated processing stages. Similarly, the coherent integration gain has been set independently of the effectiveness of the techniques implemented to enable the exploited integration times, against typical migration effects of the targets of interest. In practice, several factors could limit the performance of the conceived sensor with respect to the above expectations. Therefore, an experimental validation is essential to demonstrate the suitability of a DVB-T based PR in the airport terminal area scenario.

### III. EXPERIMENTAL TESTS AND DATA PROCESSING

#### A. Test campaigns

Dedicated acquisition campaigns have been carried out in November and December 2018 at the military airport of Pratica di Mare (Italy), using the DVB-T band AULOS® PR developed by Leonardo S.p.A..

The exploited illuminator of opportunity is a DVB-T transmitter located in Monte Cavo, approx. 22.5 km from the receiver site (see the acquisition geometry in Fig. 1(a)), while

the DVB-T-based PR receiver was installed very close to the runway of the airport (see Fig. 2(a)). Two Yagi-Uda surveillance antennas were employed with main beam width of about  $36^\circ$ . They were aligned in the horizontal plane at a distance  $d=0.63$  m

As shown in Fig. 2(b), a very small drone (DJI Phantom 4 Pro) of size approx. 25 cm x 25 cm was used as cooperative target. It was equipped with a GPS receiver that continuously recorded its position. During the test campaign, two different test area have been considered. In the first one, the drone flew in front of the RX location (gray shadowed area in Fig. 2 (a)). In the second case, the drone flew at approx. 2 km away from the RX (yellow shadowed area in Fig. 2 (a)). In both cases, the surveillance antennas have been appropriately pointed in order to include in the main beam the small flying object.

During the test campaigns, several datasets have been collected, each composed by sequential data files (namely scans). In this paper, we report the results of two datasets. The total number of scans and the temporal duration of each scan, along with other details, are reported in Table 2. In both datasets, the signals of the DVB-T channel at carrier frequency  $f_c = 570$  MHz have been collected. The GPS trajectory of the cooperative drone during the considered datasets is reported in Fig. 2(a) (black lines).

In the first dataset, the drone moved near the PR location with a maximum distance of 0.6 km (test area 1 in Fig. 2(a)). In the second dataset, the drone was at about 2 km from the receiver (test area 2 in Fig. 2(a)). For Dataset2, live air traffic control registrations have been also collected by means of an ADSB (Automatic Dependent Surveillance – Broadcast) receiver.

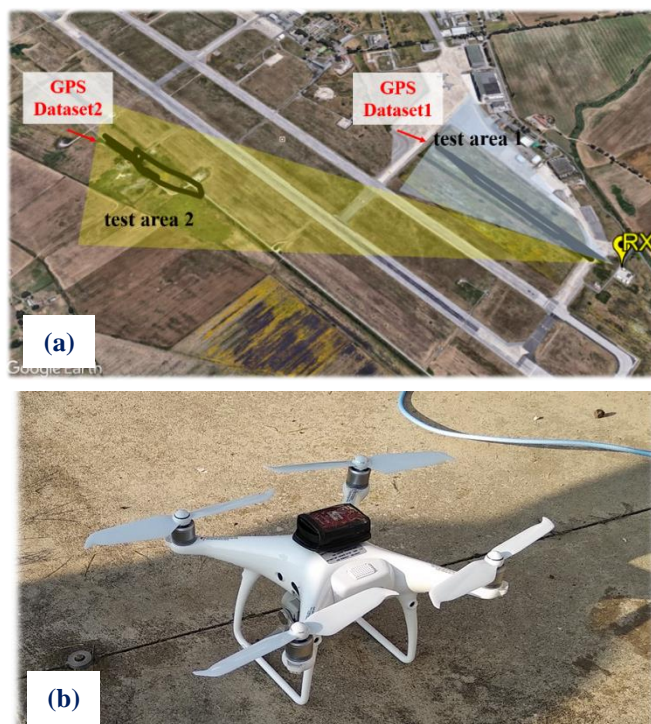


Fig. 2 – Experimental scenario: (a) sketch of the test area; (b) picture of the drone used as cooperative target.

Table 2 - Details of the data sets collected during the performed tests campaigns.

Dataset #	N° of scan	Scan duration	Total time duration	Test area
1	75	2.1 s	6 min	Test area 1
2	147	1.4 s	7 min	Test area 2

### B. DVB-T based PR processing scheme

All the available data files have been separately processed according to the DVB-T based PR processing scheme developed by the authors and described in [3],[7]. In detail, the collected data samples are simultaneously fed as input to two parallel processing chains, each one tailored to maximize the performance against the cooperative drone and the civil air traffic at farther ranges (see Fig. 3). The two processing chains feature the same main blocks. However, both the algorithms implemented in each block and the relevant parameters are properly adapted to the considered application as briefly described below.

**Disturbance cancellation.** First, a disturbance cancellation stage is performed in order to remove the direct signal, clutter and multi-path contributions. To this aim, in both cases, we adopt the sliding version of the extensive cancellation algorithm (ECA-S), [13]. Notice that, batches of small dimensions are required against aerial targets in order to synthesize a wide Doppler cancellation notch to effectively remove the disturbance. In contrast, aiming at the detection of slowly moving objects with low RCS, longer batches are to be preferred to yield a narrower cancellation notch thus preserving the target echo. Therefore, aiming at long range aerial surveillance, the ECA-S operates over a range of 33 km with a batch duration  $T_B=0.1$  s and a filter update rate  $T_S=0.6$  ms. Instead, the ECA-S operates over a range of 6 km with  $T_B=0.2$  s and  $T_S=5.2$  ms within the processing chain devoted to the detection of drones. We recall that  $T_S$  is selected in order to move out of the Doppler range of interest the undesired structures that arise from the batch processing of the received signals, [13].

**Range/Velocity map evaluation.** Then, the output of the cancellation stage and the reference signal are used in order to evaluate the bistatic range-velocity map. To this purpose, a properly filtered reference signal is employed in order to remove the high side-lobes and spurious peaks appearing in the DVB-T signal ambiguity function. To this end, we use the approach proposed in [14]. Incidentally we observe that such approach is not strictly required in the short range case since the spurious peaks appears outside the observed region. However, the mismatching described in [14] can be applied once against the reference signal that is then exploited in both the processing chains. This also guarantees that the surveillance range/Doppler area observed in short range applications is not affect by

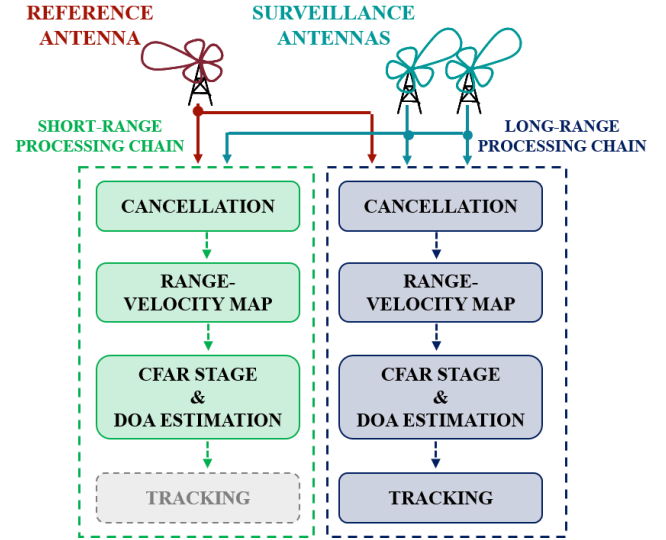


Fig. 3 – DVB-T based processing scheme for simultaneous detection and localization of drones and aircrafts.

undesired structures arising from the presence of strong targets outside that area.

The two different surveillance applications require different range-velocity map algorithms and  $T_{int}$  values. In fact, aiming at air surveillance application, long  $T_{int}$  should be exploited to extend the coverage area. Therefore, we use a  $T_{int}=1.2$  s, corresponding to the maximum allowed integration time given the data file temporal duration of 1.4 s (see Dataset2 in Table 2). Moreover, with this choice, the range walk effects have to be compensated for, by means of the approach proposed in [7]. In contrast, when short range surveillance is sought, due to the non-linear motion and the sudden accelerations of such targets, we consider a conservative solution by setting  $T_{int}=0.5$  s and we exploited the optimum Correlation FFT algorithm for range/Doppler map formation (namely, no compensation is performed of migration effects), [7].

**Detection/Localization/Tracking.** Once the range-velocity maps have been evaluated at both surveillance channels, a conventional Cell Average Constant False Alarm Rate (CA-CFAR) threshold is separately applied to each map to detect targets with a  $P_{fa} = 10^{-3}$ . Then a two-out-of-two criterion is adopted to integrate the detection results obtained at the two surveillance channels allowing a nominal  $P_{fa} = 10^{-6}$  on the final range-velocity plane. Since two surveillance antennas are available, an interferometric approach is used to estimate the direction of arrival (DoA) of the detected target echo. Finally, the bistatic range and the DoA information are converted into local Cartesian coordinates. Moreover, in the aerial scenario, a tracking stage has been applied, based on a conventional Kalman filter, in order to reduce the false alarms while yielding more accurate measurements. This stage has not been applied against drones as they are characterized by a more complex and unpredictable motion, so that advanced tracking algorithms must be considered.

## IV. EXPERIMENTAL RESULTS

Fig. 4(a)-(b) report an enlarged view of the range-velocity maps obtained for the same data file, i.e. a single scan from Dataset2. Specifically we show the maps portions around the positions of targets of interest, as extracted from the available air-truth based on GPS/ADS-B registrations (see red lines). Fig. 4(a) refers to the cooperative drone while Fig. 4(b) focuses on a civil aircraft. Notice that, all the reported maps have been scaled by the thermal noise power level so that each value represents the estimated SNR.

As is apparent, at the time of the selected scan, the drone was flying at approx. 3 km bistatic range and it yields a high SNR peak of approx. 21 dB on the corresponding range/velocity map that is clearly visible around the drone GPS track (Fig. 4 (a)). Simultaneously, a well-focused peak with  $\text{SNR} \approx 12.5$  dB is present at very long-range, at the bistatic location [235.6 km, 108.7 m/s], which is likely to correspond to the aircraft return (see Fig. 4 (b)). Notice that, the experimental target SNR values are well in line with the theoretical ones of Fig. 1.

In Fig. 5(a), we report the raw detection results over the bistatic range-velocity plane obtained for the first dataset along the whole acquisition time (6 min). Notice that, for Dataset1, since the air traffic ADS-B based air-truth is not available, we report only the short-range results. Moreover, being the duration of each scan equal to 2.1s and having set  $T_{int} = 0.5$  s, multiple scans are obtained from each data file allowing an increased number of targets observations.

In particular, in Fig. 5(a), the grey dots represent the raw detections of the PR sensor while in black is reported the available drone GPS trajectory for direct comparison. Eventually, the red dots are the correct target detections, namely the detections that correlates with the GPS. As is apparent, the system is able to detect with a good continuity the drone along its trajectory despite its small size. This is further confirmed in Fig. 6(a) where we report the raw detection results obtained for the second dataset across 75 consecutive scans. Despite the drone is at greater distance than in the first dataset, it is continuously detected. In fact, the number of correct detections is equal to 55 (over 75).

The corresponding localization results are shown in Figs. 5-6(b) overlying the Google Earth map of the local area. In order to reduce the number of false alarms, a scan-to-scan correlator has been applied on the raw detection results of Figs. 5-6(a). In Figs. 5-6(b), the grey dots correspond to the PR localization results for all the plots that survived the scan-to-scan correlation while the red plots are the ones associated to the available GPS (black trajectory). As is apparent, in both cases, the drone is localized with reasonable accuracy. In fact, a good agreement is visible between the available air truth and the PR results.

It is worth mentioning that improved results could be obtained by applying an advanced tracking stage able to handle the complex motion characteristics of the considered targets.

The simultaneous long-range detection results obtained for the second dataset are shown in Fig.7. As for Fig. 5-6(a), the grey plots are the raw detection results while in black we report the ADS-B data for comparison. Differently, the red dots are the

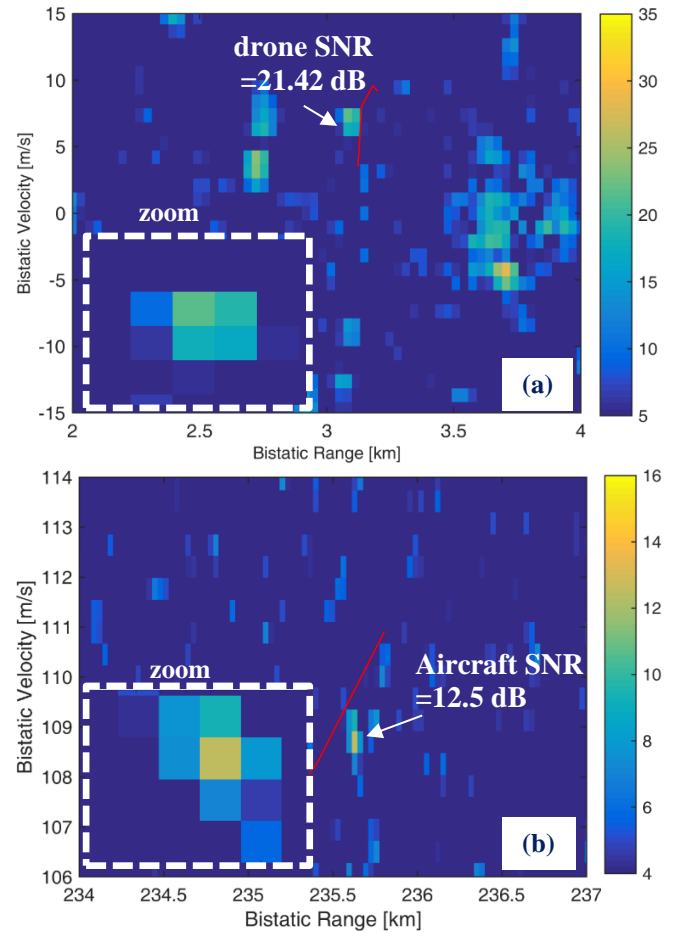


Fig. 4 – Dataset2: Enlarged view of the bistatic range-velocity maps obtained at the same scan against: (a) drone; (b) aircraft.

output of the tracking stage. We notice that targets up to 80 km of bistatic range are detected with a remarkable continuity. Moreover, the system is able to detect with a great continuity many targets also at very long bistatic ranges, up to 240 km. As it is evident, in addition to the target tracks, also ghost targets tracks (see green arrows) are present due to the single frequency network (SFN) transmission mode. Obviously, proper strategies can be adopted to suppress the ghost tracks formation 0.

## V. CONCLUSIONS

In this paper, we show the capability of the DVB-T based AULOS® PR for simultaneous short and long range surveillance of drones and aircrafts. For the purpose, an airport terminal area surveillance application has been considered. The reported results have shown the effectiveness of the sensor of simultaneously detecting and localizing a very small drone flying in the surrounding area of the airport as well as the conventional civil air traffic up to few hundreds of kilometers.

## REFERENCES

- [1] K. E. Olsen and H. Kuschel, "From the editors of the special issue: Passive and multi-static radar for civil applications," in *IEEE Aerospace and Electronic Systems Magazine*, vol. 32, no. 2, pp. 3-3, February 2017.

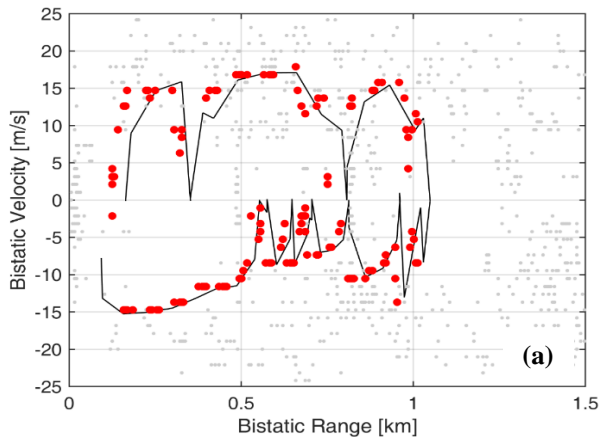


Fig. 5 - Dataset1: (a) Detection results over the Range-velocity plane; (b) Localization results on Google Earth.

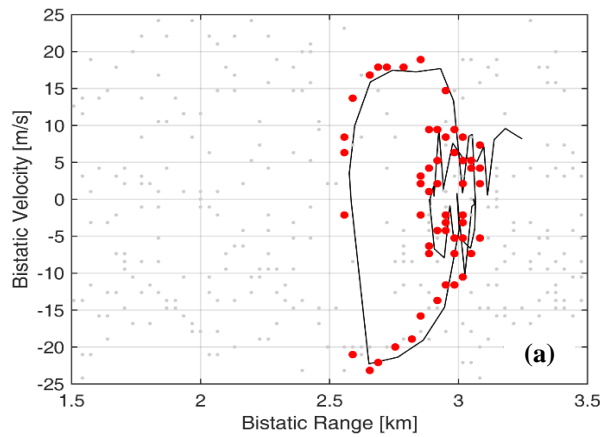


Fig. 6 – Dataset2: (a) Detection results over the Range-velocity plane; (b) Localization results on Google Earth.

- [2] D. W. O'Hagan *et al.*, "Passive Bistatic Radar (PBR) for harbour protection applications," *IEEE Radar Conference 2012*, Atlanta, GA, 2012, pp. 0446-0450.
- [3] T. Martelli, F. Colone, E. Tilli, and A. Di Lallo, "Multi-Frequency Target Detection Techniques for DVB-T Based Passive Radar Sensors," in *Sensors 2016*, Sept. 2016.
- [4] T. Martelli, F. Colone, R. Cardinali, "Eco-friendly dual-band AULOS® passive radar for air and maritime surveillance applications," *IEEE Intern. Conference on Environmental Engineering 2018*, Milan, 2018, pp. 1-6.
- [5] <https://www.newscientist.com/article/2190096-drones-are-causing-airport-chaos-why-cant-we-stop-them/>.
- [6] D. Poullin and M. Flecheux, "Passive 3D tracking of low altitude targets using DVB (SFN Broadcasters)," in *IEEE Aerospace and Electronic Systems Magazine*, vol. 27, no. 11, pp. 36-41, November 2012.
- [7] F. Pignol, F. Colone and T. Martelli, "Lagrange-Polynomial-Interpolation-Based Keystone Transform for a Passive Radar," in *IEEE Trans. on AES*, vol. 54, no. 3, pp. 1151-1167, June 2018.
- [8] Y. Liu, X. Wan, H. Tang, J. Yi, Y. Cheng and X. Zhang, "Digital television based passive bistatic radar system for drone detection," *IEEE Radar Conference 2017*, Seattle, WA, 2017, pp. 1493-1497.
- [9] D. Poullin, "Countering illegal UAV flights: passive DVB radar potentiality," *International Radar Symposium 2018*, Bonn, pp. 1-10.
- [10] M. P. Jarabo-Amores *et al.*, "Drone detection feasibility with passive radars," *European Radar Conference 2018*, Madrid, Spain, pp. 313-316.
- [11] J. Palmer, H. Harms, S. Searle, L. Davis, "DVB-T passive radar signal processing" *IEEE Trans. on Signal Proc.*, 2013, 61 (8), pp. 2116-2126.
- [12] M. I. Skolnik, Ed., *Introduction to Radar Systems*, 3rd ed. New York, NY, USA: McGraw-Hill, 2001.

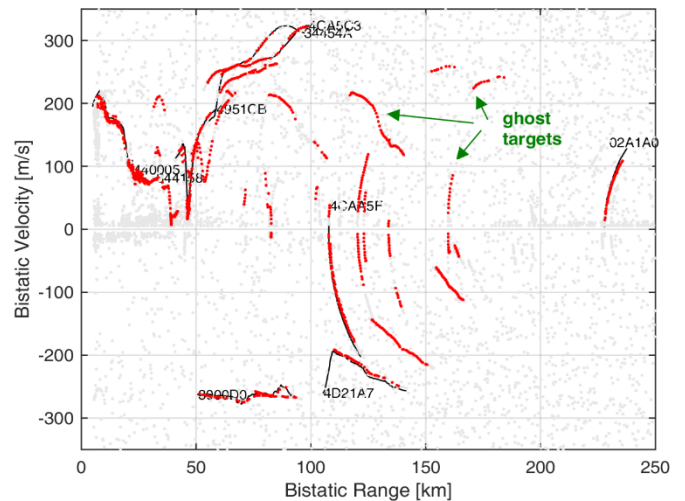


Fig. 7 - Dataset2: Long-range detection results.

- [13] F. Colone, C. Palmirini, T. Martelli, E. Tilli, "Sliding extensive cancellation algorithm for disturbance removal in passive radar," in *IEEE Trans. on AES*, vol. 52, no. 3, pp. 1309-1326, June 2016.
- [14] F. Colone, D. Langellotti, and P. Lombardo, "DVB-T signal ambiguity function control for passive radars," in *IEEE Transactions on Aerospace and Electronic Systems*, vol. 50, no. 1, pp. 329-347, January 2014.
- J. Yi, X. Wan, F. Cheng, Z. Zhao and H. Ke, "Deghosting for target tracking in single frequency network based passive radar," in *IEEE Trans. on AES*, vol. 51, no. 4, pp. 2655-2668, Oct. 2015.